Molecular Pharmacology Fast Forward. Published on May 4, 2006 as doi:10.1124/mol.105.020644

MOL #20644

Allosteric Interactions Required for High Affinity Binding of Dihydropyridine Antagonists to $Ca_V1.1$ Channels are Modulated by Calcium in the Pore

Blaise Z. Peterson and William A. Catterall

Department of Cellular and Molecular Physiology

The Penn State Milton S. Hershey College of Medicine

Hershey, PA 17033 (B.Z.P)

Department of Pharmacology

University of Washington

Seattle, WA 98195-7280 (W.A.C)

Molecular Pharmacology Fast Forward. Published on May 4, 2006 as DOI: 10.1124/mol.105.020644
This article has not been copyedited and formatted. The final version may differ from this version.

a) **Running title:** Modulation of L-type calcium channels by dihydropyridines

b) **Corresponding Author**: Blaise Z. Peterson, Ph.D.

Cellular and Molecular Physiology, H166

Penn State Milton S. Hershey Medical Center

College of Medicine

500 University Drive, Room C6603

P.O. Box 850

Hershey, PA, 17033-0850

Office: 717-531-8569 FAX: 717-531-7667

bpeterson@psu.edu

c) **Document statistics:**

1) **Number of Text Pages**: 18
2) **Number of Tables**: 2
3) **Number of Figures**: 6
4) **Number of References**: 36
5) **Number of Words in Abstract**: 250
6) **Number of Words in Introduction**: 904
7) **Number of Words in Discussion**: 1470

d) **Abbreviations:** DHP, dihydropyridine; EEEE locus, selectivity filter

Molecular Pharmacology Fast Forward. Published on May 4, 2006 as DOI: 10.1124/mol.105.020644
This article has not been copyedited and formatted. The final version may differ from this version.

ABSTRACT

Dihydropyridines (DHPs) are an important class of drugs, used extensively in the treatment of angina pectoris, hypertension, and arryhythmia. The molecular mechanism by which DHPs modulate Ca^{2+} channel function is not known in detail. We have found that DHP binding is allosterically coupled to Ca^{2+} binding to the selectivity filter of the skeletal muscle Ca^{2+} channel $Ca_V1.1$, which initiates excitation-contraction coupling and conducts L-type Ca^{2+} currents. Increasing Ca^{2+} concentrations from approximately 10 nM to 1 mM causes the DHP receptor site to shift from a low-affinity state to a high-affinity state with an EC_{50} for Ca^{2+} of 300 nM. Substituting each of the four negatively-charged glutamate residues that form the ion selectivity filter with neutral glutamine or positively-charged lysine residues results in mutant channels whose DHP binding affinities are decreased up to 10-fold and are up to 150-fold less sensitive to Ca^{2+} than wild-type channels**.** Analysis of mutations of amino acid residues adjacent to the selectivity filter led to identification of Phe-1013 and Tyr-1021, whose mutation causes substantial changes in DHP binding. Thermodynamic mutant cycle analysis of these mutants demonstrates that Phe-1013 and Tyr-1021 are energetically coupled when a single Ca^{2+} ion is bound to the channel pore. We propose that DHP binding stabilizes a nonconducting state containing a single Ca^{2+} ion in the pore through which Phe-1013 and Tyr-1021 are energetically coupled. The selectivity filter in this energetically coupled high-affinity state is blocked by bound Ca^{2+}, which is responsible for the high-affinity inhibition of Ca^{2+} channels by DHP antagoinsts.

Molecular Pharmacology Fast Forward. Published on May 4, 2006 as DOI: 10.1124/mol.105.020644
This article has not been copyedited and formatted. The final version may differ from this version.

Ca^{2+} entry through voltage-gated Ca^{2+} channels initiates a variety of cellular processes, including neurotransmitter release, muscle contraction and gene expression. Voltage-gated Ca^{2+} channels are heteromultimeric complexes consisting of α_1, β, γ and α_2/δ subunits. The α_1 subunit is the pore-forming subunit and contains the key structural determinants required for gating, drug binding and ion permeation (Fig. 1A). Ca^{2+} channels of the Ca_V1 subfamily conduct L-type Ca^{2+} currents and are the target proteins for a number of drugs including the dihydropyridines (DHPs). DHPs are allosteric modulators of channel gating, and may act as either agonists favoring an *open* state (Brown *et al.* 1984; Hess *et al.* 1984; Kokubun and Reuter 1984; Thomas *et al.* 1985; Sanguinetti *et al.* 1986) or antagonists favoring *closed* states of the channel (Bean 1984; Sanguinetti and Kass 1984; Gurney *et al.* 1985; Kokubun *et al.* 1986; Cohen and McCarthy 1987; Hamilton *et al.* 1987). While it is clear that DHPs modulate channel gating mechanisms, the molecular basis for DHP action is still not known.

Localizing the DHP receptor site was an important first step towards elucidating the mechanism by which DHPs modulate Ca^{2+} channel gating. Nine key residues important for drug binding and unique to DHP-sensitive channels were localized to transmembrane segments IIIS5, IIIS6 and IVS6 (Mitterdorfer *et al.* 1996; Peterson *et al.* 1996; Schuster *et al.* 1996; He *et al.* 1997; Peterson *et al.* 1997). When these nine L-type specific amino acids are substituted into a DHP-insensitive α_1 subunit, the resulting channel becomes sensitive to both DHP agonists and antagonists (Hockerman *et al.* 1997; Ito *et al.* 1997; Sinnegger *et al.* 1997). These studies indicate that the DHP receptor site is formed by transmembrane segments IIIS5, IIIS6 and IVS6 (Fig. 1A, *dark cylinders*).

Molecular Pharmacology Fast Forward. Published on May 4, 2006 as DOI: 10.1124/mol.105.020644
This article has not been copyedited and formatted. The final version may differ from this version.

The Ca^{2+} channel pore contains a Ca^{2+} binding site consisting of one negatively charged glutamate residue from each domain, which collectively form the selectivity filter (Fig. 1). The selectivity filter is thought to consist of a negatively charged locus capable of binding a single Ca^{2+} with high affinity or two Ca^{2+} ions with low affinity (Hille 2001; Sather and McCleskey 2003). In the absence of divalent cations, Ca^{2+} channels are highly permeable to monovalent cations. Under such conditions, Ca^{2+} ions function as channel blockers with an IC_{50} in the sub-μM range. Monovalent currents are blocked by Ca^{2+} ions because monovalent cations are unable to dislodge tightly bound Ca^{2+} ions from the selectivity filter. Currents carried by Ca^{2+} ions appear when Ca^{2+} is raised to the mM range because repulsive forces from a second Ca^{2+} ion entering the pore increase the exit-rate of the bound Ca^{2+} ion by more than 10,000-fold at physiological Ca^{2+} concentration (Almers and McCleskey 1984; Hess and Tsien 1984; Yue and Marban 1990). The original two-site barrier model nicely simulates most of the permeation properties of the channel, but it has limited value when applied to structural studies. However, the primary features of this model (i.e. binding and repulsion) almost certainly are the dominant forces in a conducting pore. Binding and repulsion of ions within the selectivity filter is a core feature of recent models of the pore that are based more on structure than the original two-site models (Dang and McCleskey 1998; Nonner *et al.* 1998; Boda *et al.* 2001; Corry *et al.* 2001; Lipkind and Fozzard 2001).

Previously, we and others found that high affinity DHP binding is dependent on Ca^{2+} binding to the selectivity filter (Mitterdorfer et al. 1995; Peterson and Catterall 1995). These findings establish an important link between DHP binding to its receptor site deep within the lipid bilayer and Ca^{2+} binding to the selectivity filter in the outer pore. This

Molecular Pharmacology Fast Forward. Published on May 4, 2006 as DOI: 10.1124/mol.105.020644
This article has not been copyedited and formatted. The final version may differ from this version.

relationship offers a unique opportunity to gain a deeper knowledge of the molecular basis for DHP action, ion permeation and gating. We have developed allosteric binding model, we systematically characterize the DHP and Ca^{2+} binding characteristics of Ca^{2+} channels whose pore-forming glutamate residues have been replaced by glutamine or lysine. We have developed an allosteric binding model that enables us to determine 1) the actual dissociation constants for Ca^{2+} binding to the selectivity filter at any DHP concentration; 2) the dissociation constant for DHP binding at any Ca^{2+} concentration; and 3) two allosteric factors that couple DHP and Ca^{2+} binding. We used this model to systematically characterize the DHP and Ca^{2+} binding characteristics of Ca^{2+} channels whose pore-forming glutamate residues have been replaced by glutamine or lysine. We find that all four of the glutamate residues that form the ion selectivity filter are important for DHP and Ca^{2+} binding. Mutational analysis of several non-glutamate residues in the outer pore revealed altered DHP- and Ca^{2+}-sensitivity, as well. Thermodynamic mutant cycle analysis (Carter *et al.* 1984; Hidalgo and MacKinnon 1995) of two of these mutants, F1013G and Y1021K, indicate that Phe-1013 and Tyr-1021 are energetically coupled when a single Ca^{2+} ion is bound in the selectivity filter, suggesting that DHP binding promotes structural rearrangements in the outer pore that involve the energetic coupling of Phe-1013 and Tyr-1021 via a single bound Ca^{2+} ion. We discuss our findings in the context of current theoretical models for permeation (Nonner *et al.* 1998; Boda *et al.* 2001; Corry *et al.* 2001; Lipkind and Fozzard 2001; Wang *et al.* 2005) and propose that DHPs block monovalent and divalent currents by stabilizing a nonconducting blocked state that is structurally and functionally analogous to a channel with a single Ca^{2+} ion in its selectivity filter.

Molecular Pharmacology Fast Forward. Published on May 4, 2006 as DOI: 10.1124/mol.105.020644
This article has not been copyedited and formatted. The final version may differ from this version.

MATERIALS AND METHODS

Preparation of wild-type and mutant $Ca_V1.1$ membranes. Wild-type and mutant α_{1S} ($Ca_V1.1$) Ca^{2+} channels were co-expressed with the β_{1a} and $\alpha_2\delta$ subunits as described previously (Peterson and Catterall 1995). Briefly, cDNAs encoding all the channel subunits, were cotransfected into tsA-201 cells by calcium phosphate precipitation and membranes were harvested 2-3 days following transfection. Cells were washed twice in Buffer A (50 mM Tris, 100 μM phenylmethylsulfonyl fluoride, 100 μM benzamidine 1.0 μM pepstatin A, 1.0 μg/μl leupeptin, and 2.0 μg/ml aprotinin, pH 8.0). Cells were scraped and homogenized in the same buffer using a glass-tephlon homogenizer. The homogenate was centrifuged at 1700 x g for 10 min and the resulting pellet was discarded. The supernatant was centrifuged at 100,000 x g for 30 min and the resulting membrane pellet was washed and homogenized in Buffer A. Membrane aliquots remained stable for several months, but were typically used within one week of harvesting.

Radioligand binding. Saturation binding assays were performed in Buffer A using 20-100 μg of membrane protein, 0.1-10 nM (+)-[3H]PN200-110 (NEN Dupont), and the indicated concentrations of free Ca^{2+} for 120 min at 22 °C. Nonspecific binding was determined by the addition of 1 μM (±)PN200-110, thus reducing k_{on} for the radio-

Molecular Pharmacology Fast Forward. Published on May 4, 2006 as DOI: 10.1124/mol.105.020644
This article has not been copyedited and formatted. The final version may differ from this version.

labeled ligand to an insignificant level, and bound radioligand was recovered by vacuum filtration using GF/C glass fiber filters.

Experiments that measure the Ca^{2+}-dependence of (+)-[^{3}H]PN200-110 binding were performed on membranes prepared from cells expressing wild-type and mutant Ca^{2+} channels. Membranes were incubated in Buffer A containing (+)-[^{3}H]PN200-110 at a concentration producing an occupancy of 0.5 in optimal Ca^{2+} (i.e., equal to the dissociation constant for (+)-[^{3}H]PN200-110 for that channel determined by saturation binding in 1 mM free Ca^{2+}), and the indicated concentrations of free Ca^{2+}. Free Ca^{2+} was buffered by the addition of 5 mM EDTA, 5 mM HE-EDTA and 5 mM nitrilotriacetic acid, and the amounts of $CaCl_2$ required to yield the desired concentrations of free Ca^{2+} determined using the Ca^{2+}-buffering calculator, MAXC (Chris Patton, Stanford University).

Data analysis. DHP binding as a function of Ca^{2+} concentration was fit using an allosteric binding model (see Fig. 2B, *Scheme 1*) described in the text with the aid of the analysis and graphics programs EXCEL (Microsoft) and ORIGIN (OriginLab Corporation). The statistical significance of the observed differences between the binding parameters of wild-type and mutant channels was evaluated using a 2-tailed Students-*t* test and ANOVA (Fig. 3). Data are means ± SEM and statistical significance was set at $P<0.05$ (*).

Molecular Pharmacology Fast Forward. Published on May 4, 2006 as DOI: 10.1124/mol.105.020644
This article has not been copyedited and formatted. The final version may differ from this version.

RESULTS

An allosteric binding model describes the positive cooperativity between DHP and Ca^{2+} binding. The DHP receptor site can exist in multiple affinity states depending on the level of Ca^{2+} present (Glossmann et al. 1985; Mitterdorfer et al. 1995; Peterson and Catterall 1995). In Fig. 2A, membranes derived from cells expressing the wild-type skeletal muscle Ca^{2+} channel ($Ca_V1.1$) were tested for binding using the DHP antagonist (+)-[^{3}H]PN200-110 in the presence of the indicated concentrations of free Ca^{2+}. Increasing the free Ca^{2+} from less than 10 nM to 100 μM causes a substantial increase in the level of (+)-[^{3}H]PN200-110 binding with an EC_{50} of approximately 0.33 μM, followed by a reduction in binding with an IC_{50} of more than 100 mM. We previously described these observations using an *Allosteric Model* where a single DHP receptor site can exists in one of three interconvertible affinity states with 0, 1, or 2 divalent cations bound to the channel (Peterson and Catterall 1995). We later found that this model could not adequately describe our experimental data. For example, the EC_{50} values measured in our Ca^{2+}-response experiments are dependent on the concentration of DHP used in the experiment—increasing DHP levels shift the EC_{50} to the left and decreasing DHP levels shift the EC_{50} to the right. Therefore, we revised this model such that it is now thermodynamically constrained and better describes the allosteric behavior of our system (Fig. 2B; *Scheme 1*). This revised version of Scheme 1 is superior to its predecessor for three main reasons: 1) the actual dissociation constants for Ca^{2+} binding to the selectivity filter at any DHP concentration can now be determined; 2) two of the three independent dissociation constants for DHP binding have been eliminated; and 3) two coupling factors, α and β, have been introduced that couple DHP and Ca^{2+} binding. Using this

Molecular Pharmacology Fast Forward. Published on May 4, 2006 as DOI: 10.1124/mol.105.020644
This article has not been copyedited and formatted. The final version may differ from this version.

revised version of *Scheme 1*, we are now able to quantitatively assess the binding affinity for Ca^{2+} to the channel and the cooperativity between the Ca^{2+} and DHP receptor sites. It turns out that α, which was completely absent in the original model, is altered in several of the most interesting mutant channels assessed in these studies (see below).

Scheme 1 is thermodynamically constrained such that the ratio of dissociation constants for DHP binding in the absence and presence of Ca^{2+} must equal to the ratio of the dissociation constants for Ca^{2+} binding in the absence and presence of DHP. Therefore, the individual dissociation constants for DHP and Ca^{2+} binding are completely determined by K_{D1} and K_{C1}, respectively, and the allosteric factors α and β. This expression of *Scheme 1* allows one to determine the individual dissociation constants for Ca^{2+} binding in the absence and presence of a DHP ligand (Tables 1 and 2).

Ca^{2+} binding to the outer pore is allosterically coupled to DHP binding. The pore segments from each domain of DHP-sensitive ($Ca_V1.1$-4) and –insensitive ($Ca_V2.1$-3) Ca^{2+} channels are aligned in Fig. 1B. To determine whether Ca^{2+} binding to the pore is allosterically coupled to DHP binding, each of the negatively charged glutamate residues that collectively form the selectivity filter (Fig. 1B, *boxes*) was replaced by a neutral glutamine or a positively charged lysine residue, generating the mutants E292Q, E614Q, E1014Q, E1323Q, E292K, E614K, E1014K and E1323K. E614K and E1323K exhibited no DHP binding and were not studied further. K_{D1} for each mutant was determined by saturation binding in the presence of 1 mM free Ca^{2+} and increasing concentrations of (+)-[^{3}H]PN200-110. K_{D1} values for wild-type and each of the mutant channels are summarized in Fig. 3A and Table 1. The sensitivity of the wild-type and mutant channels

Molecular Pharmacology Fast Forward. Published on May 4, 2006 as DOI: 10.1124/mol.105.020644
This article has not been copyedited and formatted. The final version may differ from this version.

to Ca^{2+} was determined by incubating membranes in a concentration of (+)-[^{3}H]PN200-110 equal to the measured K_{D1} value for that particular channel (resulting in an occupancy of 0.5) plus increasing concentrations of free Ca^{2+}, as described in the Materials and Methods. K_{C1} and α were determined by fitting these data using *Scheme 1*, with K_{D1} and free (+)-[^{3}H]PN200-110 serving as fixed parameters. K_{D1}, K_{C1} and α for wild-type and each mutant channel are summarized in Fig. 3 and Table 1.

DHP binding, the sensitivity of DHP binding to Ca^{2+} and the coupling factor α are altered for the mutant channels. The values determined for K_{D1}, the dissociation constant for DHP binding to a channel whose selectivity filter is occupied by a single Ca^{2+} ion, are increased 5.5- to 10-fold by these mutations (Fig. 3A; Table 1). Although the four glutamate residues are not contiguously localized on the primary sequence, each functions as an important DHP binding determinant in the presence of Ca^{2+}, suggesting that the selectivity filter acts as a unified locus that modulates DHP binding. Nevertheless, mutations of the four glutamate residues affect K_{D1}, K_{C1} and α to different extents. These differences indicate that the binding site for Ca^{2+} ions is asymmetrical, as is the coupling of each glutamate residue to DHP binding (Fig. 3).

As expected for mutant channels with amino acid substitutions in their selectivity filters, dramatic changes in K_{C1}, the dissociation constant for Ca^{2+} binding to DHP-occupied Ca^{2+} channels, were observed (Fig. 3B). The smallest change in K_{C1} was observed with E292Q, whose binding of Ca^{2+} is reduced by less than 12-fold. The other glutamate mutants exhibited reductions in affinity for Ca^{2+} from 90 to 150-fold.

The allosteric coupling factor α, which reflects the effect of binding of one Ca^{2+} ion on DHP affinity, was reduced from 15.5 for wild-type to values ranging from 1.3 to 9.8

Molecular Pharmacology Fast Forward. Published on May 4, 2006 as DOI: 10.1124/mol.105.020644
This article has not been copyedited and formatted. The final version may differ from this version.

for the glutamate substitution mutants (Fig. 3C). E292Q, whose value for α was *increased* to 54.5, was the only exception to this trend. The role α plays in determining DHP binding properties is discussed in greater detail, below. Together, the changes in K_{D1}, K_{C1} and α in these mutants indicate that the DHP receptor site is allosterically coupled to the selectivity filter of L-type Ca^{2+} channels. Therefore, it is plausible that the molecular details that underlie DHP activity may involve structural rearrangements in the outer pore and selectivity filter of the channel.

Uncharged residues in the outer pore are critical for DHP and Ca^{2+} binding. A comparison of the amino acid sequences in the outer pore segments of each repeat of the Ca^{2+} channel isoforms reveals several residues that are unique to DHP-sensitive channels and are adjacent to the Ca^{2+}-binding glutamate residues in the selectivity (Fig. 1B). To determine whether these residues are important DHP- and/or Ca^{2+}-binding determinants, the mutants C288A, F1013G, Q1018E, Q1018M, Y1021K, C1319A, Q1326H and E1327Q were constructed and analyzed as described above and in the Materials and Methods (Fig. 4; Table 2). C288A, Q1018E, Q1018M, C1319A, Q1326H and E1327Q have DHP- and Ca^{2+}-binding profiles similar to those of wild-type and are not discussed further.

In contrast to the glutamate mutants, high affinity binding of DHP and Ca^{2+} is enhanced for mutant F1013G, in which a Gly characteristic of Ca_V2 channels is substituted for Phe in $Ca_V1.1$. K_{D1} for F1013G is slightly lower than that of wild-type (0.22 verses 0.31 nM, respectively), and K_{C1} for F1013G decreased 2.3-fold from 40 nM to 17.4 nM (Fig. 4A and B). However, the most interesting change in the binding profile

Molecular Pharmacology Fast Forward. Published on May 4, 2006 as DOI: 10.1124/mol.105.020644
This article has not been copyedited and formatted. The final version may differ from this version.

for F1014G is the 12.5-fold increase in magnitude of the coupling factor, α, which results in an 11-fold increase in αK_{D1} compared to wild-type (Fig. 4C).

High-affinity binding of DHP and Ca^{2+} is also modified for mutant Y1021K, in which a Lys characteristic of $Ca_V2.1$ and $Ca_V2.2$ channels is substituted for Tyr in $Ca_V1.1$ (Fig. 4). First, in contrast to F1013G, K_{D1} for Y1021K is three-fold larger than K_{D1} for wild-type (Fig. 4A; Table 2). Second, K_{C1} for Y1021K is more than 30-fold larger than K_{C1} for wild-type (Fig. 4B). Finally, while the coupling factor α for F1013G is 12.5-fold larger than that of wild-type, α for Y1021K is only half that of wild-type (Fig. 4C).

The results with F1013G and Y1021K indicate that non-glutamate residues in the outer pore loop function as important binding determinants for DHPs and Ca^{2+} ions. The qualitative differences in the effects of these mutations on ligand binding suggest that the roles Phe-1013 and Tyr-1021 play in DHP and Ca^{2+} binding are distinct.

Ca^{2+} promotes energetic coupling between Phe-1013 and Tyr-1021. Qualitatively divergent effects of Ca^{2+} on DHP binding affinity were observed with the mutants F1013G and Y1021K (Fig. 4; Table 2), even though these two substitutions typically coexist in Ca_V2 channels within nine amino acid residues in the outer pore loop of domain III (Fig. 1B). This prompted us to construct a mutant channel in which Phe-1013 and Tyr-1021 have been replaced with Gly and Lys, respectively, resulting in the double mutant FY/GK. The double mutation causes a much larger increase in K_{D1} than either single mutation (Fig. 4A, Table 2), whereas the values of K_{C1} and α are intermediate between the two single mutants (Fig. 4B, C, Table 2). Thus, the parameters for DHP and Ca^{2+} binding to FY/GK differ substantially from the sum of those for the single mutants,

Molecular Pharmacology Fast Forward. Published on May 4, 2006 as DOI: 10.1124/mol.105.020644
This article has not been copyedited and formatted. The final version may differ from this version.

indicating that the two residues interact energetically in their function as DHP and Ca^{2+} binding determinants.

Thermodynamic mutant cycle analysis (Carter *et al.* 1984; Hidalgo and MacKinnon 1995) was used to quantitate the energetic interaction between Phe-1013 and Tyr-1021 in DHP binding (Fig. 5). The coupling energy between Phe-1013 and Tyr-1021 was calculated in nominally zero Ca^{2+} using αK_{D1} values (Fig. 5A) and in 1 mM Ca^{2+} using K_{D1} values (Fig. 5B) by subtracting the $\Delta\Delta G$ that results from replacing Phe-1013 with Gly in a wild-type background from the $\Delta\Delta G$ that results from the same substitution made in a Y1021K background. These analyses demonstrate that the degree of coupling between Phe-1013 and Tyr-1021 in DHP binding is highly dependent on the occupancy of the selectivity filter by Ca^{2+}. The coupling energy in nominally zero Ca^{2+} of 0.08 kcal/mol is negligible (Fig. 5A). This near-zero coupling energy indicates that, in the absence of Ca^{2+} (i.e., state [α_1] of *Scheme 1*), Phe-1013 and Tyr-1021 are not energetically coupled. In contrast, the coupling energy between Phe1013 and Tyr-1021 determined in 1 mM Ca^{2+} is substantial. Replacing Phe-1013 with Gly is highly dependent on whether the substitution is placed in a wild-type backbone (+0.22 kcal/mol) versus the Y1021K backbone (-1.23 kcal/mol). Therefore, when the selectivity filter is occupied by a single Ca^{2+} ion (i.e., state [Ca/α_1] of *Scheme 1*), Phe-1013 and Tyr-1021 are strongly coupled with an energy of 1.45 kcal/mol [(+0.22 kcal/mol) – (-1.23 kcal/mol) = 1.45 kcal/mol]. This 'coupled state', in which Phe-1013 and Tyr-1021 are energetically coupled and a single Ca^{2+} ion is bound, may represent a stably blocked, nonconducting state of the channel, as addressed in the discussion below.

Molecular Pharmacology Fast Forward. Published on May 4, 2006 as DOI: 10.1124/mol.105.020644
This article has not been copyedited and formatted. The final version may differ from this version.

The coupling factor α plays an important role in determining the Ca^{2+}-dependence of DHP binding. The effects of the coupling factor, α, on the Ca^{2+}-dependence of DHP binding to the mutant Ca^{2+} channels are illustrated in Fig. 6. These relationships between DHP binding affinity (K_{D1}^{-1} and αK_{D1}^{-1} in nM^{-1}) and Ca^{2+} concentration were simulated from the binding model in *Scheme 1* and the binding parameters from Table 1. The DHP affinity of E292Q is 11-fold less than that of wild-type with no Ca^{2+} ions bound to selectivity filter, but due to a 3.5-fold increase in α compared to wild-type, the affinity is decreased by only 3-fold when one Ca^{2+} ion is bound (Fig. 6A). In contrast to E292Q, α values for the other glutamate mutants are smaller than those of wild-type (Fig. 3). Consequently, the increases in DHP affinity upon binding of a single Ca^{2+} ion to these mutants are much less than for E292Q or wild-type, as illustrated for E292K in Fig. 6A. In the absence of Ca^{2+}, the DHP binding affinity for mutants E1014K and E1014Q are nearly identical to that of wild-type (Fig. 6B). Increasing Ca^{2+} concentration has even less effect on DHP binding for E1014Q and E1014K (Fig. 6B) than for E292Q (Fig. 6A).

The largest change in the magnitude of α was observed with mutant F1013G, whose value for α is 12.5-fold greater than that of wild-type (Table 2). While the affinity of mutant F1013G for DHPs is more than 11-fold lower than wild-type in the absence of Ca^{2+}, there is little difference in DHP binding affinity between wild-type and F1013G when one Ca^{2+} ion is bound (Fig. 6C). In contrast, the affinity for DHP binding of Y1021K is similar to wild-type in the absence of Ca^{2+} but 3-fold less than wild-type when one Ca^{2+} ion is bound. This difference in the effect of Ca^{2+} on DHP binding to F1013G and Y1021K results from the 12.5-fold increase in α observed for F1013G

Molecular Pharmacology Fast Forward. Published on May 4, 2006 as DOI: 10.1124/mol.105.020644
This article has not been copyedited and formatted. The final version may differ from this version.

compared to the 2-fold decrease in α for Y1021K. Overall, these comparisons illustrate that the coupling factor α is a key determinant of the effect of Ca^{2+} on DHP binding and of DHP affinity under physiological conditions.

DISCUSSION

Ca^{2+} binding to the pore of the L-type Ca^{2+} channels is allosterically coupled to DHP binding, which suggests that the binding of DHPs and Ca^{2+} promotes reciprocal structural rearrangements in the outer pore that alter the functional behavior of the channel. To better understand the roles amino acid residues residing in the outer pore have on DHP binding, permeation and gating, the binding properties of 16 mutant Ca^{2+} channels were assessed using *Scheme 1*. In addition to dramatic changes in the dissociation constants for DHP and Ca^{2+} binding, we found that the coupling factor α plays a major role in determining the pharmacological properties of the mutant channels. For example, α for the non-glutamate mutant F1013G is increased nearly 200-fold, while α for Y1021K is only half that of wild-type. Thermodynamic mutant cycle analysis of these mutants indicates that Phe-1013 and Tyr-1021 are energetically coupled only when the outer pore is occupied by a single Ca^{2+} ion. Our findings are discussed in the context of current theoretical models for permeation (Nonner *et al.* 1998; Boda *et al.* 2001; Lipkind and Fozzard 2001; Wang *et al.* 2005). We propose that DHPs block monovalent and divalent currents by stabilizing a nonconducting blocked state that is structurally and functionally analogous to a channel with a single Ca^{2+} ion in its selectivity filter.

Molecular Pharmacology Fast Forward. Published on May 4, 2006 as DOI: 10.1124/mol.105.020644
This article has not been copyedited and formatted. The final version may differ from this version.

Binding of DHP antagonists and Ca^{2+} stabilize a blocked conformation of the outer pore. In the absence of Ca^{2+}, the outer pore is held in an *open* conformation ($[\alpha_1]$) by electrostatic repulsion between the four glutamate residues of the EEEE locus. When a single Ca^{2+} ion enters the selectivity filter, it acts as a counter charge and draws the four glutamate residues together to form a *blocked* conformation ($[Ca/\alpha_1]$) (Lipkind and Fozzard 2001). According to *Scheme 1*, DHP binding interacts allosterically with Ca^{2+} to stabilize the *blocked* conformation thereby preventing Ca^{2+} conductance. Neutralizing any one of the four glutamate residues would destabilize this *blocked* conformation by reducing the magnitude of the attractive forces between the bound Ca^{2+} ion and the partially-neutralized selectivity filter. In Fig. 3, the K_{D1} values for the glutamate-to-glutamine mutants are all larger than wild-type. Neutralization of the residues in the selectivity filter would destabilize the *open* conformation of the outer pore as well, because the magnitude of the repulsive forces between the four glutamate residues would be decreased. The simulations in Fig. 6 show reduced DHP binding in the absence of Ca^{2+}, indicating that this postulate holds true.

Introduction of positively charged lysine residues mimics binding of Ca^{2+}. Replacing the substituted glutamine residues with positively-charged lysine residues would be expected to partially mimic a Ca^{2+} ion by acting as a countercharge in the selectivity filter. If the charge-reversal substitutions were to perfectly mimic a single bound Ca^{2+} ion in the pore, αK_{D1} would equal K_{D1} and the coupling factor α would equal 1. We were pleased to find that the charge-reversal substitutions did follow this predicted trend but as might be expected, inserting a lysine with a valence of only +1 into a

Molecular Pharmacology Fast Forward. Published on May 4, 2006 as DOI: 10.1124/mol.105.020644
This article has not been copyedited and formatted. The final version may differ from this version.

constrained position in the selectivity filter does not perfectly mimic a free divalent Ca^{2+} ion in the pore. The affinity for DHP binding in nominal Ca^{2+} (i.e., $1/\alpha K_{D1}$) to E292K and E1014K membranes is 3- and 2-fold higher than their charge-neutralized counterparts (Fig. 6). These findings indicate that the introduction of a positive charge in the selectivity filter makes the *[α_1]* state of the outer pore behave more like the Ca^{2+}-bound *[Ca/α_1]* state.

The charge-reversal mutants are still sensitive to Ca^{2+}, but the fold-change in binding affinity that occurs as the channel transitions from *[α_1]* to *[Ca/α_1]* (i.e., the coupling factor, α) is reduced. This reduction occurs because replacing the neutral glutamine residues with positively charged lysine residues introduces repulsive forces between the positively-charged amine of the lysine residue and the incoming Ca^{2+} ion. Consequently, α values for E292K and E1014K are decreased 8.5- and 3.3-fold compared to their glutamine-substituted counterparts. The combined effects on αK_{D1} and α indicate that the introduction of a positive charge in the pore partially mimics a single Ca^{2+} ion coordinated in the selectivity filter.

Mechanism for DHP action. The cooperativity between DHP and Ca^{2+} binding suggests that DHPs modulate channel gating by promoting conformational changes in the outer pore. We used a 'volume exclusion/charge neutralization' model to explain the reduced conductance of Ba^{2+} but not Ca^{2+} through the pores of $Ca_V1.2$ correlates of F1013G, Y1021K and FY/GK (Wang et al. 2005). The crystal diameters of Ca^{2+} and Na^+ ions are nearly identical (2.00 versus 2.04 angstroms, respectively), yet each Ca^{2+} ion carries twice as much counter-charge as a Na^+ ion. Therefore, Ca^{2+} binds tightly to the

Molecular Pharmacology Fast Forward. Published on May 4, 2006 as DOI: 10.1124/mol.105.020644
This article has not been copyedited and formatted. The final version may differ from this version.

selectivity filter because it is able to neutralize the highly charged EEEE locus without overcrowding it with counter-ions. Ba^{2+} and Ca^{2+} ions carry the same charge, but the ionic diameter of Ba^{2+} is approximately 36% larger than that of Ca^{2+}. Thus, Ba^{2+} ions exhibit a higher degree of crowding, lower binding affinity and consequential faster exit-rate (i.e., larger conductance) than Ca^{2+} ions. These results suggest that Ba^{2+} conductance is reduced because Ba^{2+} ions in mutant pores are less prone to overcrowding.

According to *Scheme 1*, Ca^{2+}- and DHP- binding shifts the configuration of the outer pore from an *open* state to a *blocked* state. [α_1] or [2Ca/α_1] are designated as conducting states in *Scheme 1* because they represent channels conducting monovalent and divalent currents, respectively. The *blocked* state, [Ca/α_1] is designated as a nonconducting state because single Ca^{2+} ions are known to block both monovalent and divalent (i.e., Ba^{2+}) currents (Almers et al. 1984; Hess and Tsien 1984; Hille 2001). Here, we combine the 'volume exclusion/charge neutralization' model with *Scheme 1* and propose that DHPs block mono- and di-valent currents through the *open* [α_1] and [2Ca/α_1] states of the outer pore by stabilizing a non-conducting *blocked* state that is structurally and functionally analogous to [Ca/α_1].

This postulate is consistent with the structural model of Lipkind and Fozzard. In this model, the eight carboxyl groups from the EEEE locus are thought to form three binding sites: a central high affinity divalent cation binding site formed by four carboxyl groups flanked by two low affinity sites, each composed of two carboxyl groups (Lipkind and Fozzard, *Biochemistry* 40:6786, 2001). Divalent cation permeation through such a pore would depend on the occupancy of the two low affinity sites, thus producing a conducting state ([2Ca/α_1]). Ion permeation would be prevented if the central, high

Molecular Pharmacology Fast Forward. Published on May 4, 2006 as DOI: 10.1124/mol.105.020644
This article has not been copyedited and formatted. The final version may differ from this version.

affinity site were occupied by a single Ca^{2+} ion, thus producing a non-conducting state ([Ca/α_1]). In the absence of divalent cations, repulsive forces in the EEEE locus would open the pore to greater than four Å and allow the passage of monlvalent cations through the pore, thus producing a conducting state for monovalent cations ([α_1]).

Given this scenario, the outer pore of an activated channel would switch between conducting ([2Ca/α1]) and nonconducting, blocked ([Ca/α_1]) states. The overall P_O of a channel would be determined by the probability that the inner gate is open and the probability that the channel is in state [Ca/α_1], which is dependent on the dwell time of the single blocking Ca^{2+} ion residing in the selectivity filter. We propose that DHP antagonists increase this dwell-time and that the P_O of the channel decreases as a consequence. It will be interesting to use single-channel measurements to determine whether the mean open times decrease in the presence of DHP antagonists. Unfortunately, these experiments are quite challenging using $Ca_V1.1$ channels, so this hypothesis will be tested using the cardiac $Ca_V1.2$ channel.

Energetic coupling mediated by bound Ca^{2+}. The conformational changes that underlie the transitions between the *open* and *blocked* states of the outer pore modulate DHP binding affinity dependent on the magnitude of the coupling factor α. We used thermodynamic mutant cycle analysis to assess the transition of the outer pore between the *open* and *blocked* states, [α_1] and [Ca/α_1], respectively. Our results demonstrate that Phe-1013 and Tyr-1021 are strongly coupled only when the selectivity filter is occupied by a single Ca^{2+} ion but not when the selectivity filter is unoccupied by Ca^{2+} (Fig. 2B, *Scheme 1*; *box*). Evidently, the bound Ca^{2+} ion serves to mediate energetic coupling

Molecular Pharmacology Fast Forward. Published on May 4, 2006 as DOI: 10.1124/mol.105.020644
This article has not been copyedited and formatted. The final version may differ from this version.

between these two aromatic amino acid residues, which are located on either side of Glu-1014 (Fig. 1). This coupling may result from electronic interactions between the two aromatic residues through the bound Ca^{2+} ion, structural rearrangements in the selectivity filter caused by Ca^{2+} binding, or both. We postulate that Phe-1013 and Tyr-1021 are energetically coupled when the pore is in a *blocked*, nonconducting state, and that DHP antagonists block the channel by stabilizing this same nonconducting conformational state. The positive energetic coupling between Phe-1013 and Tyr-1021 revealed here is likely to make a major contribution to the stability of this Ca^{2+}-bound, blocked state.

Molecular Pharmacology Fast Forward. Published on May 4, 2006 as DOI: 10.1124/mol.105.020644
This article has not been copyedited and formatted. The final version may differ from this version.

ACKNOWLEDGEMENTS

We thank Gregory M. Lipkind for his insightful comments on this manuscript.

Molecular Pharmacology Fast Forward. Published on May 4, 2006 as DOI: 10.1124/mol.105.020644
This article has not been copyedited and formatted. The final version may differ from this version.

REFERENCES

Almers, W. and E. W. McCleskey (1984). Non-selective conductance in calcium channels of frog muscle: calcium selectivity in a single-file pore. *J Physiol* **353**: 585-608.

Almers, W., E. W. McCleskey and P. T. Palade (1984). A non-selective cation conductance in frog muscle membrane blocked by micromolar external calcium ions. *J Physiol* **353**: 565-83.

Bean, B. P. (1984). Nitrendipine block of cardiac calcium channels: high-affinity binding to the inactivated state. *Proc Natl Acad Sci U S A* **81**(20): 6388-92.

Boda, D., D. Henderson and D. D. Busath (2001). Monte Carlo simulations of the mechanism for channel selectivity: the competition between volume exclusion and charge neutrality. *J. Phys. Chem* **104**: 11574-11577.

Brown, A. M., D. L. Kunze and A. Yatani (1984). The agonist effect of dihydropyridines on Ca channels. *Nature* **311**(5986): 570-2.

Carter, P. J., G. Winter, A. J. Wilkinson and A. R. Fersht (1984). The use of double mutants to detect structural changes in the active site of the tyrosyl-tRNA synthetase (Bacillus stearothermophilus). *Cell* **38**(3): 835-40.

Cohen, C. J. and R. T. McCarthy (1987). Nimodipine block of calcium channels in rat anterior pituitary cells. *J Physiol* **387**: 195-225.

Corry, B., T. W. Allen, S. Kuyucak and S. H. Chung (2001). Mechanisms of permeation and selectivity in calcium channels. *Biophys J* **80**(1): 195-214.

Dang, T. X. and E. W. McCleskey (1998). Ion channel selectivity through stepwise changes in binding affinity. *J Gen Physiol* **111**(2): 185-93.

Glossmann, H., D. R. Ferry, A. Goll, J. Striessnig and G. Zernig (1985). Calcium channels and calcium channel drugs: recent biochemical and biophysical findings. *Arzneimittelforschung* **35**(12A): 1917-35.

Gurney, A. M., J. M. Nerbonne and H. A. Lester (1985). Photoinduced removal of nifedipine reveals mechanisms of calcium antagonist action on single heart cells. *J Gen Physiol* **86**(3): 353-79.

Hamilton, S. L., A. Yatani, K. Brush, A. Schwartz and A. M. Brown (1987). A comparison between the binding and electrophysiological effects of dihydropyridines on cardiac membranes. *Mol Pharmacol* **31**(3): 221-31.

He, M., I. Bodi, G. Mikala and A. Schwartz (1997). Motif III S5 of L-type calcium channels is involved in the dihydropyridine binding site. A combined radioligand binding and electrophysiological study. *J Biol Chem* **272**(5): 2629-33.

Hess, P., J. B. Lansman and R. W. Tsien (1984). Different modes of Ca channel gating behaviour favoured by dihydropyridine Ca agonists and antagonists. *Nature* **311**(5986): 538-44.

Hess, P. and R. W. Tsien (1984). Mechanism of ion permeation through calcium channels. *Nature* **309**(5967): 453-6.

Hidalgo, P. and R. MacKinnon (1995). Revealing the architecture of a K+ channel pore through mutant cycles with a peptide inhibitor. *Science* **268**(5208): 307-10.

Hille, B. (2001). Ion channels of excitable membranes. Sunderland, MA, Sinaur Associates, Inc.

Hockerman, G. H., B. Z. Peterson, E. Sharp, T. N. Tanada, T. Scheuer and W. A. Catterall (1997). Construction of a high-affinity receptor site for dihydropyridine agonists

and antagonists by single amino acid substitutions in a non-L- type Ca2+ channel. *Proc Natl Acad Sci U S A* **94**(26): 14906-11.

Ito, H., N. Klugbauer and F. Hofmann (1997). Transfer of the high affinity dihydropyridine sensitivity from L-type To non-L-type calcium channel. *Mol Pharmacol* **52**(4): 735-40.

Kokubun, S., B. Prod'hom, C. Becker, H. Porzig and H. Reuter (1986). Studies on Ca channels in intact cardiac cells: voltage-dependent effects and cooperative interactions of dihydropyridine enantiomers. *Mol Pharmacol* **30**(6): 571-84.

Kokubun, S. and H. Reuter (1984). Dihydropyridine derivatives prolong the open state of Ca channels in cultured cardiac cells. *Proc Natl Acad Sci U S A* **81**(15): 4824-7.

Lipkind, G. M. and H. A. Fozzard (2001). Modeling of the outer vestibule and selectivity filter of the L-type Ca2+ channel. *Biochemistry* **40**(23): 6786-94.

Mitterdorfer, J., M. J. Sinnegger, M. Grabner, J. Striessnig and H. Glossmann (1995). Coordination of Ca2+ by the pore region glutamates is essential for high-affinity dihydropyridine binding to the cardiac Ca2+ channel alpha 1 subunit. *Biochemistry* **34**(29): 9350-5.

Mitterdorfer, J., Z. Wang, M. J. Sinnegger, S. Hering, J. Striessnig, M. Grabner and H. Glossmann (1996). Two amino acid residues in the IIIS5 segment of L-type calcium channels differentially contribute to 1,4-dihydropyridine sensitivity. *J Biol Chem* **271**(48): 30330-5.

Nonner, W., D. P. Chen and B. Eisenberg (1998). Anomalous mole fraction effect, electrostatics, and binding in ionic channels. *Biophys J* **74**(5): 2327-34.

Peterson, B. Z. and W. A. Catterall (1995). Calcium binding in the pore of L-type calcium channels modulates high affinity dihydropyridine binding. *J Biol Chem* **270**(31): 18201-4.

Peterson, B. Z., B. D. Johnson, G. H. Hockerman, M. Acheson, T. Scheuer and W. A. Catterall (1997). Analysis of the dihydropyridine receptor site of L-type calcium channels by alanine-scanning mutagenesis. *J Biol Chem* **272**(30): 18752-8.

Peterson, B. Z., T. N. Tanada and W. A. Catterall (1996). Molecular determinants of high affinity dihydropyridine binding in L- type calcium channels. *J Biol Chem* **271**(10): 5293-6.

Sanguinetti, M. C. and R. S. Kass (1984). Voltage-dependent block of calcium channel current in the calf cardiac Purkinje fiber by dihydropyridine calcium channel antagonists. *Circ Res* **55**(3): 336-48.

Sanguinetti, M. C., D. S. Krafte and R. S. Kass (1986). Voltage-dependent modulation of Ca channel current in heart cells by Bay K8644. *J Gen Physiol* **88**(3): 369-92.

Sather, W. A. and E. W. McCleskey (2003). Permeation and selectivity in calcium channels. *Annu Rev Physiol* **65**: 133-59.

Schuster, A., L. Lacinova, N. Klugbauer, H. Ito, L. Birnbaumer and F. Hofmann (1996). The IVS6 segment of the L-type calcium channel is critical for the action of dihydropyridines and phenylalkylamines. *Embo J* **15**(10): 2365-70. abs.html.

Sinnegger, M. J., Z. Wang, M. Grabner, S. Hering, J. Striessnig, H. Glossmann and J. Mitterdorfer (1997). Nine L-type amino acid residues confer full 1,4-dihydropyridine sensitivity to the neuronal calcium channel alpha1A subunit. Role of L- type Met1188. *J Biol Chem* **272**(44): 27686-93.

Thomas, G., M. Chung and C. J. Cohen (1985). A dihydropyridine (Bay k 8644) that enhances calcium currents in guinea pig and calf myocardial cells. A new type of positive inotropic agent. *Circ Res* **56**(1): 87-96.

Wang, X., T. A. Ponoran, R. L. Rasmusson, D. S. Ragsdale and B. Z. Peterson (2005). Amino Acid Substitutions in the Pore of the CaV1.2 Calcium Channel Reduce Barium Currents without Affecting Calcium Currents. *Biophys J* **89**(3): 1731-43.

Yue, D. T. and E. Marban (1990). Permeation in the dihydropyridine-sensitive calcium channel. Multi-ion occupancy but no anomalous mole-fraction effect between Ba2+ and Ca2+. *J Gen Physiol* **95**(5): 911-39.

Molecular Pharmacology Fast Forward. Published on May 4, 2006 as DOI: 10.1124/mol.105.020644
This article has not been copyedited and formatted. The final version may differ from this version.

FOOTNOTES

* This work was supported by research grants from the American Heart Association (0230298N to B.Z.P.) and the National Institutes of Health (RO1 HL074143 to B.Z.P. and P01 HL44948 to W.A.C.)

Molecular Pharmacology Fast Forward. Published on May 4, 2006 as DOI: 10.1124/mol.105.020644
This article has not been copyedited and formatted. The final version may differ from this version.

FIGURE LEGENDS

Figure 1. The selectivity filter consists of four negatively charged glutamate residues that bind a single Ca^{2+} ion with a high affinity or two Ca^{2+} ions with a low affinity.

A. The α_1 subunit of the Ca^{2+} channel consists of four homologous repeats (I, II, III, IV) that assemble to form the pore of the channel complex. Each repeat consists of 6 transmembrane segments, S1-S6. The loops connecting the 5th and 6th transmembrane segments from each repeat contain highly conserved glutamate residues (denoted with an '*E*') that collectively form the selectivity filter. The selectivity filter is capable of binding a single Ca^{2+} ion with a high affinity or two Ca^{2+} ions with a low affinity. Dihydropyridine agonists and antagonists interact with amino acid residues located in transmembrane segments IIIS5, IIIS6 and IVS6 (*dark cylinders*). **B.** The pore segments from each of the four domains of the DHP –sensitive ($Ca_V1.1$-4) and –insensitive ($Ca_V2.1$-3) Ca^{2+} channels are aligned. The Ca^{2+}-binding glutamate residues that form the selectivity filter are indicated with *boxes*.

Figure 2. Ca^{2+} is a positive allosteric modulator of DHP binding.

A. Membranes prepared from cells expressing wild-type Ca^{2+} channels were incubated with [^{3}H]PN200-110 at a concentration equal to its dissociation constant measured in 1 mM free Ca^{2+} (1 x K_{D1}) and the indicated concentrations of free Ca^{2+} (see Materials and Methods). Data from one such experiment (*circles*) demonstrates that increasing Ca^{2+} from 10 nM to 1 mM results in a large increase in DHP binding with an EC_{50} of approximately 0.3 μM. Further increases in Ca^{2+} to the 100 mM range results in a large decrease in DHP binding with an IC_{50} in the high mM range. The line is a smooth fit

Molecular Pharmacology Fast Forward. Published on May 4, 2006 as DOI: 10.1124/mol.105.020644
This article has not been copyedited and formatted. The final version may differ from this version.

through the data points and was generated using *Scheme 1* from Panel **B.** *Scheme 1* is described in the text.

Figure 3. Ca^{2+} binding to the selectivity filter is allosterically coupled to DHP binding.

A-B. Individual dissociation constants, K_{D1} (A) and K_{C1} (B) were determined for [^{3}H]PN200-110 and Ca^{2+} binding to wild-type and the indicated mutant channels as described in the Materials and Methods. K_{D1} and K_{C1} values for all glutamine and lysine substitutions are significantly different than wild-type. K_{C1} for the glutamine substitutions in domains II, III and IV are significantly different from E292Q. K_{D1} values for E292Q and E1014Q are significantly different from E1323Q but not E614Q. **C.** Values for the coupling factor α were determined as described in the Materials and Methods using *Scheme* 1 (see also, Fig. 2A).

Figure 4. Non-glutamate residues in the pore segment of domain III are critical for DHP and Ca^{2+} binding.

A-C. Non-glutamate residues in the pores of repeats I, III and IV were altered and analyzed as described in Figure 3.

Figure 5. Ca^{2+} binding to the selectivity filter promotes energetic coupling between Phe-1013 and Tyr-1021.

Double mutant cycle analysis was used to measure the coupling energy between Phe-1013 and Tyr-1021 in the absence (**A**) and presence (**B**) of a single Ca^{2+} ion in the

Molecular Pharmacology Fast Forward. Published on May 4, 2006 as DOI: 10.1124/mol.105.020644
This article has not been copyedited and formatted. The final version may differ from this version.

selectivity filter. PN200-110 binding to its receptor site is driven by a negative change in Gibbs free energy, ΔG. ΔG changes for mutant channels whose affinity for DHP binding is altered and this change in ΔG, designated ΔΔG, is calculated using the dissociation constants for drug binding to the wild-type and mutant channels, such that: $\Delta\Delta G = -RTln(K_{Dmut}/K_{Dwt})$, where *R* is the gas constant and *T* is the absolute temperature in Kelvin. ΔΔG values (kcal/mol) for each mutant channel are noted by *numbers* adjacent to *arrows*. Thermodynamic mutant cycle analysis is based on the principle that the ΔΔG value resulting from the simultaneous alteration of two amino acids is equal to the sum of the ΔΔG values for the individual substitutions that lead to the double mutant. For example, note in Panel A that the ΔΔG for the double mutant FY/GK (–1.76 kcal/mol) is equal to the sum of the ΔΔG values for the individual steps that lead to FY/GK; i.e., [(-1.42) + (-0.34)] and [(-0.26) + (-1.50)]. The 'coupling energy' between two amino acids can be determined by calculating the difference between the ΔΔG values associated with the horizontal (or vertical) arrows as described in the text. Notice that Phe-1013 and Tyr-1021 are strongly coupled only when a single Ca^{2+} ion is bound to the selectivity filter (see also, Fig. 2B; *vertical box*).

Figure 6. Substitution of positively-charged lysine residues in the selectivity filter partially mimics a bound Ca^{2+} ion.

Simulations of [^{3}H]PN200-110 binding affinity (nM^{-1}) versus free Ca^{2+} for wild-type (*dashed lines*) and the mutants E292Q and E292K (**A**), E1014Q and E1014K (**B**) and F1013G and Y1021K (**C**) are plotted using the binding parameters from Tables 1 and 2. The expression levels of E614K and E1323K were too low to use in these analyses. Fold

Molecular Pharmacology Fast Forward. Published on May 4, 2006 as DOI: 10.1124/mol.105.020644
This article has not been copyedited and formatted. The final version may differ from this version.

differences between the DHP binding affinities of wild-type and/or mutant channels are indicated by *numbers* adjacent to *arrows*.

Table 1. The effects glutamate substitutions in the Ca^{2+} channel pore have on Ca^{2+}- and DHP- binding parameters.

	K_{D1} nM (fold-change)	αK_{D1} (nM) nM (fold-change)	K_{C1}(μM) μM (fold-change)	αK_{C1} (μM) μM (fold-change)	α (fold-change)
Wild-type	0.31±0.031	4.8±0.59	0.040±0.005	0.62±0.10	15.5±1.90
E292Q	0.93±0.15 (3) *	50.7±10 (10.6) *	0.462±0.08 (11.6) *	23.0±1.5 (37) *	54.5±11.3 (3.5) *
E614Q	2.68±1.4 (8.6) *	13.5±3.1 (2.8) *	5.83±0.83 (146) *	29.2±6.6 (47) *	5.11±1.32 (0.3)
E1014Q	1.71±0.29 (5.5) *	7.71±0.80 (1.6)	3.72±1.74 (93) *	20.6±4.1 (33) *	4.45±0.48 (0.3) *
E1323Q	2.88±0.50 (9.3) *	28.1±3.7 (5.8) *	4.05±0.10 (101) *	35.6±2.3 (57) *	9.75±1.3 (0.6)
E292K	2.69±0.73 (8.7) *	17.3±4.0 (3.6) *	6.17±1.9 (154) *	34.4±2.6 (55) *	6.40±1.5 (0.4)
E614K	n.d.	n.d.	n.d.	n.d.	n.d.
E1014K	2.98±0.68 (9.6) *	3.98±0.25 (0.8)	4.20±2.6 (105) *	5.42±3.1 (8.7) *	1.33±0.09 (0.1) *
E1323K	n.d.	n.d.	n.d.	n.d.	n.d.

Values are means±SEM. **Asterisks (*)** indicates values that are significantly different from wild-type, as determined by the Student's Independent t-test; P<0.05. Each value is determined from 3-14 experiments (see MATERIALS AND METHODS for details). n.d.; not determined.

Table 2. The effects non-glutamate substitutions in the Ca^{2+} channel pore have on Ca^{2+}- and DHP- binding parameters.

	K_{D1} nM (fold-change)	αK_{D1} (nM) nM (fold-change)	K_{C1}(μM) μM (fold-change)	αK_{C1} (μM) μM (fold-change)	α (fold-change)
Wild-type	0.31±0.031	4.8±0.59	0.040±0.005	0.62±0.10	15.5±1.90
C288A	0.25±0.02 (0.8)	3.63±0.03 (0.8)	0.075±0.01 (1.8)	1.09±0.22 (1.8)	14.5±1.0 (0.9)
F1013G *	0.22±0.01 (0.7)	42.6±10.0 (8.9) *	0.017±0.008 (0.4)	3.37±1.48 (5.4) *	194±48 (12.5)
Q1018M (0.6)	0.31±0.03 (0.0)	2.74±0.12 (0.6)	0.041±0.004 (0.0)	0.36±0.04 (0.6)	8.88±0.38
Q1018E	0.25±0.02 (0.8)	5.56±1.7 (1.2)	0.028±0.005 (0.7)	0.61±0.21 (0.0)	22.0±6.7 (1.4)
Y1021K (0.5)	0.94±0.05 (3.0) *	7.05±0.45 (1.5)	1.25±0.69 (31.3) *	9.38±5.7 (15.1) *	7.51±0.48
C1319A	0.30±0.03 (0.0)	2.85±0.08 (0.6)	0.048±0.05 (1.2)	0.45±0.03 (0.7)	9.5±0.27 (0.6)
Q1326H	0.57±0.16 (1.8)	7.40±0.71 (1.5)	0.046±0.005 (1.1)	0.60±0.12 (0.0)	13.1±1.2 (0.8)
E1327N (0.5)	0.59±0.17 (1.9)	4.77±0.13 (0.0)	0.065±0.02 (1.6)	0.53±0.17 (0.8)	8.08±0.22
FY/GK	7.51±0.92 (24.3) *	93.9±14.2 (20.6) *	0.237±0.08 (5.9) *	3.00±1.2 (4.8) *	12.5±1.9 (0.8)

Values are means±SEM. **Asterisks (*)** indicates values that are significantly different from wild-type, as determined by the Student's Independent t-test; P<0.05. Each value is determined from 3-14 experiments (see MATERIALS AND METHODS for details).

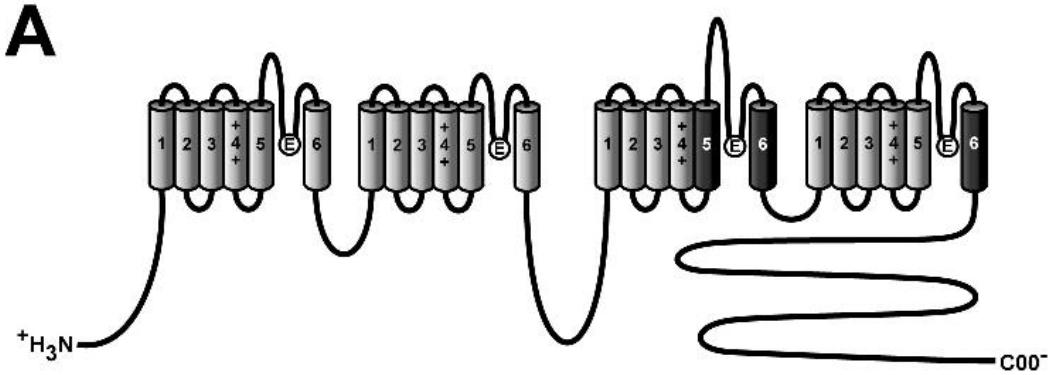

B

	Motif I	Motif II
(CaV1.1)	QCITM**E**GWTDVLYWVND	QVLTG**E**DWTSMMYNG
(CaV1.2)	QCITM**E**GWTDVLYWMQD	QILTG**E**DWNSVMYDG
(CaV1.3)	QCITM**E**GWTDVLYWMND	QILTG**E**DWNAVMYDG
(CaV1.4)	QCVTM**E**GWTDVLYWMQD	QILTG**E**DWNVVMYDG
(CaV2.1)	QCITM**E**GWTDLLYNSND	QILTG**E**DWNEVMYDG
(CaV2.2)	QCITM**E**GWTDILYNTND	QILTG**E**DWNAVMYHG
(CaV2.3)	QCITM**E**GWTTVLYNTND	QILTG**E**DWNEVMYNG

	Motif III	Motif IV
(CaV1.1)	TVSTF**E**GWPQLLYKAID	RCATG**E**AWQEILLAC
(CaV1.2)	TVSTF**E**GWPELLYRSID	RCATG**E**AWQDIMLAC
(CaV1.3)	TVSTF**E**GWPALLYKAID	RCATG**E**AWQEIMLAC
(CaV1.4)	TVSTF**E**GWPALLYKAID	RCATG**E**AWQEIMLAS
(CaV2.1)	TVSTG**E**GWPQVLKHSVD	RSATG**E**AWHNIMLSC
(CaV2.2)	TVSTG**E**GWPMVLKHSVD	RSATG**E**AWHEIMLSC
(CaV2.3)	TVSTG**E**GWPQVLQHSVD	RSATG**E**AWQEIMLSC

Figure 1

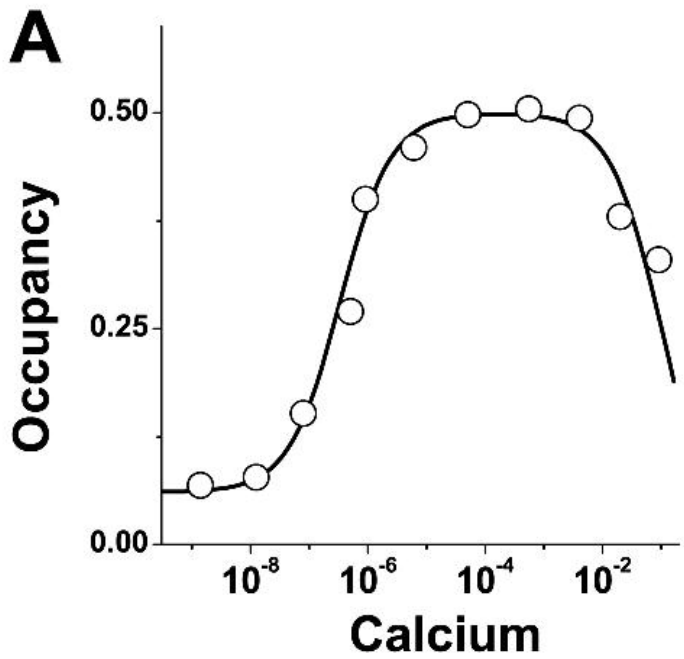
A
Occupancy
0.50
0.25
0.00
10^{-8}
10^{-6}
10^{-4}
10^{-2}
Calcium

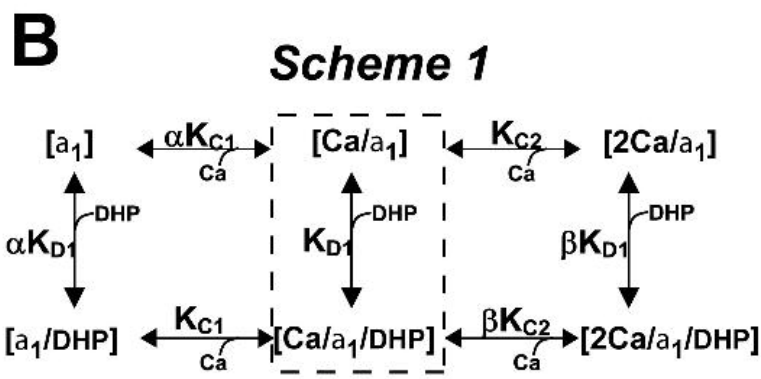
B
Scheme 1
[a1]
αKC1
Ca
[Ca/a1]
KC2
Ca
[2Ca/a1]
αKD1
DHP
KD1
DHP
βKD1
DHP
[a1/DHP]
KC1
Ca
[Ca/a1/DHP]
βKC2
Ca
[2Ca/a1/DHP]

Figure 2

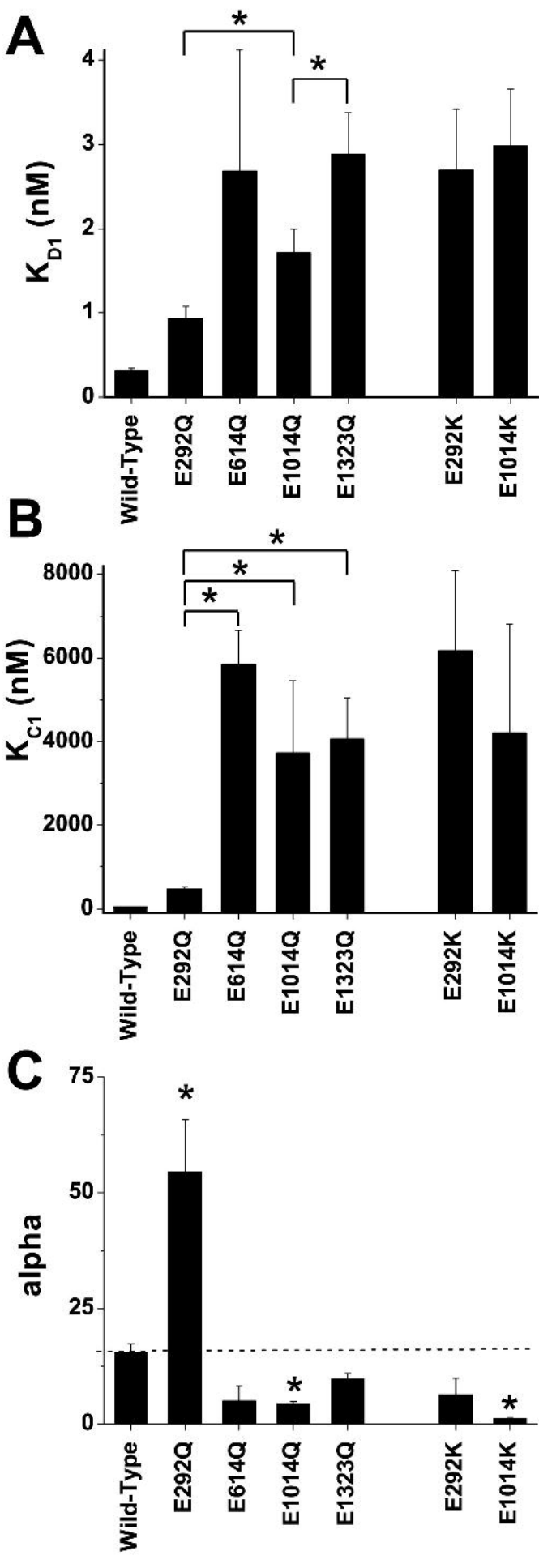
A
K_{D1} (nM)
0
1
2
3
4
*
*
B
K_{C1} (nM)
0
2000
4000
6000
8000
*
*
*
C
alpha
0
25
50
75
*
*
*
Wild-Type
E292Q
E614Q
E1014Q
E1323Q
E292K
E1014K

Figure 3

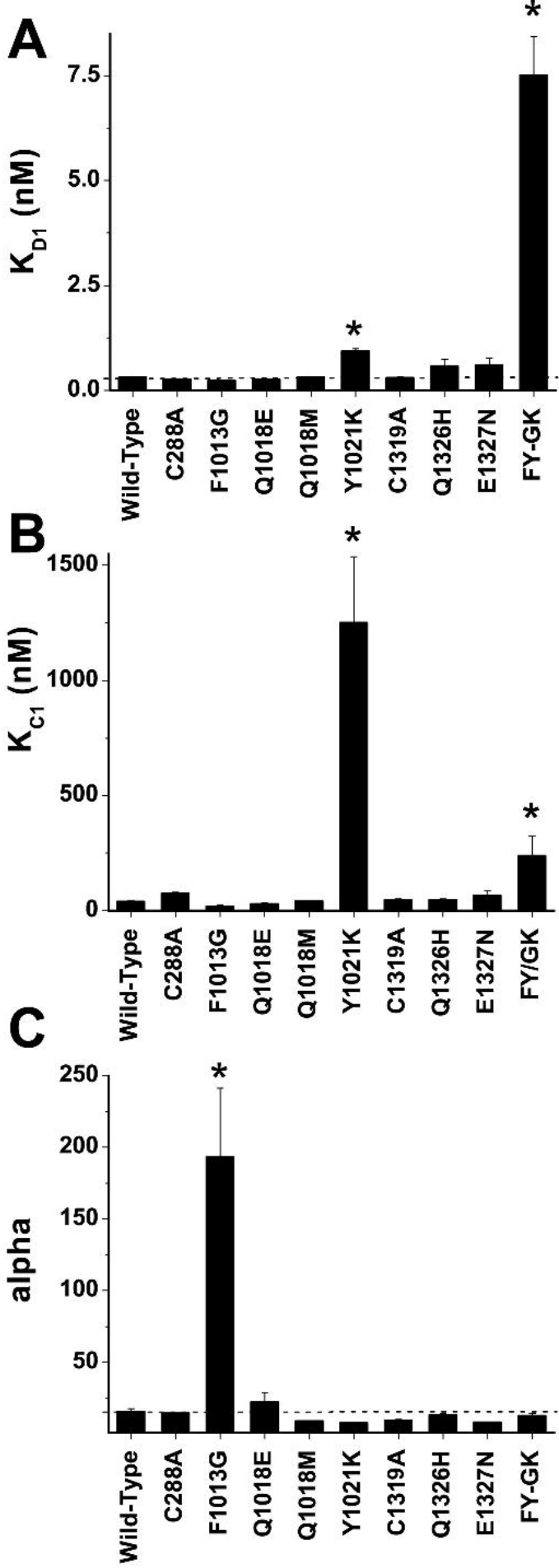
A
K_{D1} (nM)
7.5
5.0
2.5
0.0
*
*
Wild-Type
C288A
F1013G
Q1018E
Q1018M
Y1021K
C1319A
Q1326H
E1327N
FY-GK
B
K_{C1} (nM)
1500
1000
500
0
*
*
Wild-Type
C288A
F1013G
Q1018E
Q1018M
Y1021K
C1319A
Q1326H
E1327N
FY/GK
C
alpha
250
200
150
100
50
*
Wild-Type
C288A
F1013G
Q1018E
Q1018M
Y1021K
C1319A
Q1326H
E1327N
FY-GK

Figure 4

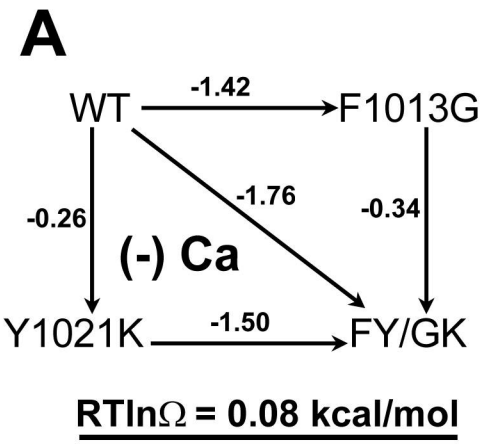
A
WT
-1.42
F1013G
-0.26
-1.76
-0.34
(-) Ca
Y1021K
-1.50
FY/GK
RTlnΩ = 0.08 kcal/mol

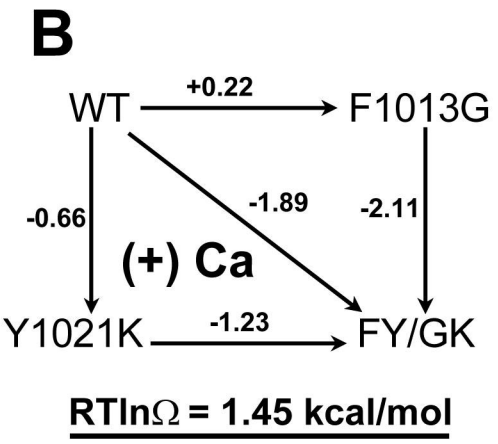
B
WT
+0.22
F1013G
-0.66
-1.89
-2.11
(+) Ca
Y1021K
-1.23
FY/GK
RTlnΩ = 1.45 kcal/mol

Figure 5

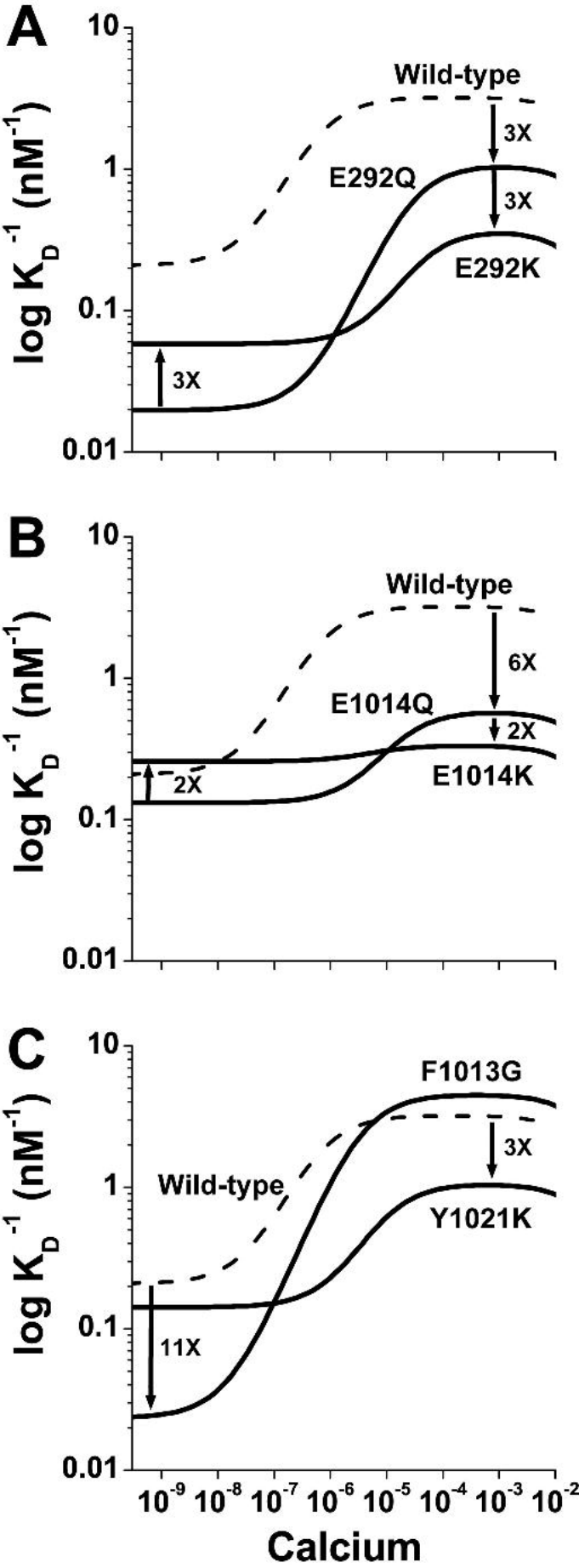
A
B
C
log K_D^{-1} (nM^{-1})
10
1
0.1
0.01
Wild-type
E292Q
E292K
3X
3X
3X
E1014Q
E1014K
6X
2X
2X
F1013G
Y1021K
11X
10^{-9} 10^{-8} 10^{-7} 10^{-6} 10^{-5} 10^{-4} 10^{-3} 10^{-2}
Calcium

Figure 6